NUMERICAL DESIGN TOOLS FOR THERMAL REPLICATION OF OPTICAL-QUALITY SURFACES

Y.M. Stokes[1]
Department of Applied Mathematics,
University of Adelaide, Adelaide, SA 5005, Australia.

[1]Facsimile: 61 8 8303 3696. Email: ystokes@maths.adelaide.edu.au

Abstract

Y.M. Stokes, Department of Applied Mathematics, University of Adelaide

The slumping of molten glass under gravity into a mould, so as to replicate the mould surface on the upper free surface of the glass, is used in the manufacture of some optical components for which the curvature of the upper free surface is critical. A finite-element simulation of the process based on the creeping-flow equations is described. In addition a method is given for computing surface curvature from the non-exact discrete data produced by the finite-element computations. These methods are illustrated for a particular case of a circular glass disc slumping into a spherical mould.

1 Introduction

Thermal replication is an industrial process used in the manufacture of aspheric optical surfaces. At present accuracy limitations restrict its application to products requiring no more than ophthalmic-optics quality [12] such as mirrors, and ophthalmic lenses and lens moulds [14]. The process is described by Smith et al.[14]. A glass workpiece, having a well polished upper surface, is placed on a ceramic mould, and this combination heated in a kiln so that the glass softens and "slumps" into the mould replicating the mould surface on its upper surface. This process is illustrated in Figure 1. The upper free surface of the glass, that does not contact the mould, is the critical optical surface. It is very smooth and requires no polishing — a difficult and costly process for complicated aspheric surfaces.

The aim of this manufacturing process is to replicate the macro-surface of the mould on the upper surface of the glass as nearly as possible, while smoothing out any small-scale imperfections in the mould surface. The upper glass surface does not, however, exactly replicate the mould surface, and consequently the design of the optical surface and its associated ceramic mould involves an iterative process of slumping, measuring the resultant glass surface, and re-cutting the mould, in order to achieve the desired optical surface

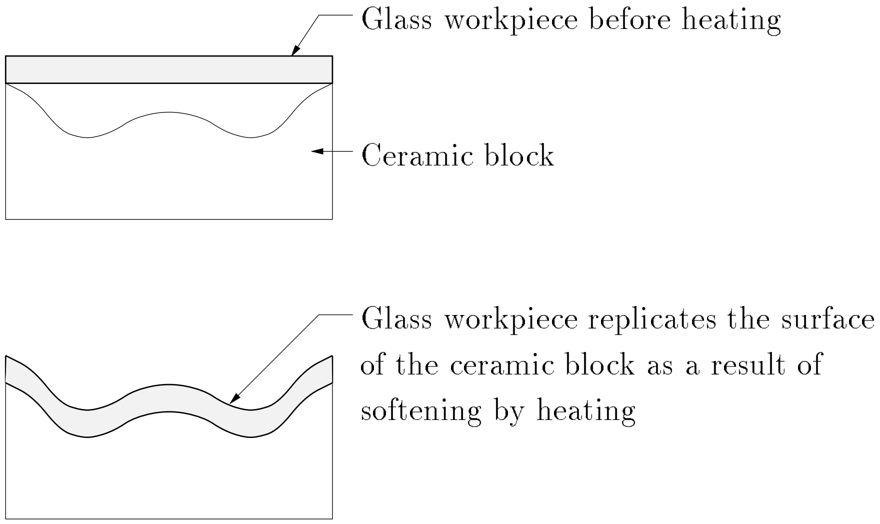

Figure 1: Thermal Replication (after Smith et al. [14])

at the required accuracy. Here the numerical modelling of this slumping process is investigated, the ultimate aim being to greatly reduce, if not eliminate, the experimental iteration currently required. Such a numerical tool would be of considerable benefit to the optics industry.

Molten glass is a very viscous fluid having a viscosity of order 10^7 Pa·s and higher, at normal slumping temperatures. Thus, flow is very slow, being characterised by a small Reynolds number, and can be modelled by the Stokes creeping-flow equations. These are solved using the finite-element method, which is the preferred numerical method for modelling of forming processes (see Preface of [11]), and is especially so where moving free-surface boundaries are involved.

The slumping of a bridge of very viscous fluid spanning the gap between two vertical no-slip walls, and involving no mould contact has been considered by Tuck et al. [17]. Similar to slumping, blow-moulding is a process where a layer of very viscous fluid is forced against a mould by creating a pressure drop across its thickness, and this has been the subject of considerable investigation with particular application to the manufacture of axisymmetric containers [4, 5, 7, 19]. In all of this work, slow-flow approximations have been made and finite-element methods employed. Asymptotic methods have also been used for pressure driven flows of thin viscous sheets without mould contact [9, 18], but are not easily extended to include mould contact.

2 Glass Properties

It is generally assumed that molten glass in the viscosity range at which moulding is done is an incompressible fluid. While this is not strictly true, it is considered to be sufficiently accurate for practical purposes, and in any case, is an assumption made in all current methods for determining molten glass viscosities [8]. Furthermore, while a viscous isotropic Maxwell fluid model was used in some early glass modelling work [5, 19], it is now generally accepted that molten glasses, with but few exceptions, are Newtonian fluids [13], and this assumption has been adopted in more recent work [4, 7, 9, 17, 18]. Thus, slumping molten glass is here assumed to be an incompressible, Newtonian flow. The density of glass does not vary much with temperature, and may be reasonably assumed to be constant. Any surface tension effects are also ignored, which is justified on the basis that the capillary number is large (see [17]).

Complex issues do however arise in the consideration of the relationship between temperature and viscosity, which must be the most important physical consideration in modelling of glass forming processes. Firstly, there is the phenomenon of relaxation and equilibrium viscosity, and secondly the viscosity of a molten glass is highly temperature sensitive.

At large viscosity, a change in temperature takes a finite time to be reflected in the corresponding change in viscosity, with this time increasing as viscosity increases (and temperature decreases). This is known as relaxation, and the final viscosity reached is called the equilibrium viscosity. With viscosity (μ) measured in decipascal seconds (or poise), Scholze and Kreidl [13] give $L = \log(\mu) = 10$ as the point at which viscosity lags by some seconds behind a fast cooling rate, and $13 \leq L \leq 14.5$ as the glass transition in which lag time varies from around 15 minutes to 4 hours and properties are most definitely time dependent. In the numerical modelling of slumping, consideration must be given to the change in glass viscosity as it is heated at the commencement of the slumping process, when viscosity is potentially higher than equilibrium. From practical experience [16] slumping will occur, given sufficient time, at viscosities as high as $L = 11$, which is just on the fringes of the time-dependent property region given in [13]. Practically however, very little slumping would occur at such high viscosities, since oven temperatures are quickly increased to bring the viscosity down into the region $7 \leq L \leq 8$ where slumping occurs at a faster and more acceptable rate, and any lag will only serve to further prevent slumping at this stage. Thus it is assumed that relaxation will not significantly affect slumping, and that computation based on equilibrium viscosities will be adequate. In any case any time lag in the viscosity can be easily corrected by adjusting the time scale as will be discussed.

The sensitivity of viscosity to temperature is an issue that is less easily dismissed. With viscosity varying by more than an order of magnitude over the slumping temperature range (about $650 - 700^{o}$C), there is a clear possibility that spatial variation of temperature throughout the molten glass may significantly affect its flow behaviour. Certainly for some processes such as blow-moulding, where a parison must first be formed and the mould is cold, spatial temperature variations are likely to be quite important, and thermal modelling should be coupled with fluid-flow modelling [4, 5, 19]. In slumping however, both mould and glass are heated together from room temperature so that spatial temperature variations will be considerably less than for blow-moulding. On the other hand, the tolerances on the quality of optical surfaces formed by slumping are necessarily very much tighter than tolerances on container wall thickness and surface finish, so that such spatial variations as do exist might still be of importance. Thus, while an isothermal model (i.e. temperature constant in space but not necessarily in time) might be adequate, there is a need to investigate spatial temperature variation.

Such an investigation is however, fraught with considerable difficulties. The commonly adopted Vogel-Fulcher-Tammann (VFT) empirically derived equation may be used to approximate the viscosity-temperature relationship of the glass [13], but this relies on being able to determine the temperature within the glass. This is by no means trivial given a general lack of information on glass thermal properties and how these vary with temperature, plus very ill-defined issues of glass-mould contact and non-uniformity of kiln temperatures. As a result, in work by others very approximate and simple thermal models have been assumed [4, 5, 19] or the isothermal case alone has been solved [7, 18], in order to get some qualitative idea of the flow behaviour.

The approach taken by this author [16] has been to develop a finite element formulation and program that enables the imposition of any temperature/viscosity distribution of possible interest, and use this to conduct sensitivity studies into the effects of spatial temperature variation on the flow of the glass. Preliminary comparisons of these with experimental slumping results [15] indicate that an isothermal model is reasonable, and hence, in this paper isothermal slumping conditions are assumed. It is worth commenting that any temporal temperature profiles are easily accommodated with an isothermal model, as will be seen.

3 A Stokes-Flow Model

The very large viscosity of molten glass and the consequent small slumping velocity scale ($\sim 1/\mu$) and Reynolds number ($\sim 1/\mu^2$) permit a quasi-steady formulation of the problem, obtained by simplifying the full Navier-Stokes flow equations to the creeping-flow or Stokes equations [3, p.216 *ff*]. These are solved for the (steady) flow applicable over a small time interval. The fluid geometry is then updated to reflect the small changes brought about by this flow, and the process repeated.

For a fluid of density ρ and viscosity μ, in a gravity field of strength g acting in the $-x_3$ direction, the equations to be solved are (in tensor notation)

$$\frac{\partial p}{\partial x_i} = \frac{\partial}{\partial x_j}\left[\mu\left(\frac{\partial u_i}{\partial x_j} + \frac{\partial u_j}{\partial x_i}\right)\right] - \rho g \delta_{3i} \tag{1}$$

together with the continuity equation for incompressible flow

$$\frac{\partial u_i}{\partial x_i} = 0. \tag{2}$$

At boundaries that are in contact with the mould the no-slip conditions

$$u_i = 0 \tag{3}$$

must be satisfied, and on all other boundaries the no-stress free-surface conditions

$$-pn_i + \mu n_j \left(\frac{\partial u_i}{\partial x_j} + \frac{\partial u_j}{\partial x_i}\right) = 0 \tag{4}$$

apply, where n_i is the unit normal. In all equations, indices i and j have range from 1 to 3 for three dimensions.

Equations (1) and (2) are solved subject to the prescribed boundary conditions (3) and (4) for velocity u_i and pressure p, using the finite-element method with a mesh of 6-node triangles over the flow domain. As is usual, linear basis functions are used for pressure and quadratic basis functions are used for velocity.

The time evolution of the flow geometry is given by solving the slumping dynamics equations

$$u_i = dx_i/dt \tag{5}$$

at each node using the known velocity field, to give the new node positions x_i. The mesh is then adjusted by moving each node to its new position, to give a new geometry on which the procedure is repeated. As slumping progresses, the lower free surface of the glass contacts the mould surface, and because of this Euler's method has been used to solve (5) for x_i at the $(n+1)$th time step:

$$x_i^{n+1} = x_i^n + u_i^n \times \Delta t. \tag{6}$$

Then a simple check can be conducted to ensure that no node crosses the mould boundary, but at best just reaches it, the time step Δt being reduced if necessary to satisfy this criterion. While a more accurate time-stepping method is possible (see discussion in [16]), this method has been found to give good accuracy provided node displacements are sufficiently small, and if necessary the time step is also reduced so that the displacement of each node does not exceed a prescribed maximum amount. When a node reaches the mould boundary its boundary conditions are changed from free-surface to no-slip. This is exactly the method of handling mould contact described in [4, 7].

Rather than work with the dimensional equations given above, the dimensionless equations are obtained by setting ρ, g and μ to unity. Dimensional quantities are given by multiplying by the appropriate scales. Choosing the disc radius a as the length scale $\mathcal{L}$, the velocity, pressure and time scales $\mathcal{U}$, $\mathcal{P}$ and $\mathcal{T}$ are given by

$$\mathcal{U} = \frac{\rho g a^2}{\mu}, \qquad \mathcal{P} = \rho g a, \qquad \mathcal{T} = \frac{\mu}{\rho g a}. \tag{7}$$

From this we see that the Reynolds number $(\rho \mathcal{U} \mathcal{L}/\mu)$ is like $1/\mu^2$ as claimed earlier.

An important consequence of the neglect of the time derivatives in the field equations (1), together with the isothermal assumption, is that temporal changes in viscosity may be accommodated by a time scale $\mathcal{T}(t)$ that varies in time with viscosity. To see this, first consider a viscosity that is everywhere and forever constant. The solution of the dimensionless field equations, (1) and (2) with $\mu = \rho = g = 1$, for flow velocity and pressure is influenced only by the flow-domain geometry at the time of solution, and not by the time itself. The finite-element mesh is then adjusted to reflect the distortion caused by flow over a dimensionless time step Δt^*, and the velocity and pressure fields are recomputed over this new geometry. After a dimensionless time t^* there is only one possible geometrical outcome from this process (ignoring numerical error caused by discrete approximation). The dimensionless time t^* over which this happens represents a real time given by $t^*\mathcal{T}$, where the time scale $\mathcal{T}$ is dependent on the constant viscosity as shown in (7). Different values of the viscosity μ mean different real slump times, but the same final outcome. Thus, the model tells us that, given identical initial geometries, the same item can be obtained by slumping at a high viscosity for a long time, or a lower viscosity for a shorter time.

Next let viscosity $\mu(t)$ be given as a function of time, and let us define a time scale that is also a function of time

$$\mathcal{T}(t) = \frac{\mu(t)}{\rho g a}\,. \tag{8}$$

In any very small real-time interval dt the viscosity is constant, and the corresponding dimensionless-time interval is given by $dt^* = dt/\mathcal{T}(t)$. Then a slumping time period of length t_f during which the viscosity is given as a function of time by $\mu(t)$ is obtained in dimensionless terms by summing over

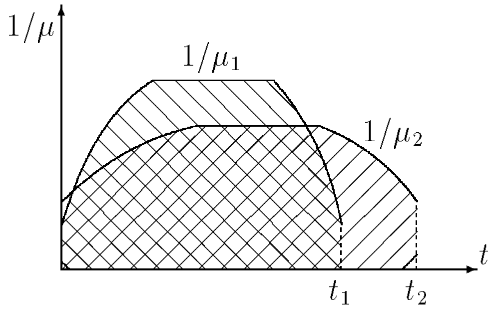

Figure 2: Equivalent Viscosity Curves

all very small intervals dt:

$$t^* = \int_0^{t_f} \mathcal{T}(t)^{-1} dt = \rho g a \int_0^{t_f} \mu(t)^{-1} dt \,. \qquad (9)$$

For constant viscosity, (9) reduces to $t^* = t_f/\mathcal{T}$, as indeed it should.

Now it is evident from (9) that a particular value of t^* can be obtained from a host of different choices of t_f and $\mu(t)$ (keeping ρ, g and $\mathcal{L}$ constant), including constant μ, and the finite-element program will for some initial geometry compute a single slumped shape for this dimensionless time. Another look at (9) shows that, provided there is equal area under each curve of inverse viscosity $\mu(t)^{-1}$, from the time at which slumping starts to the time at which it ends (see Figure 2), the final product resulting from some initial geometry will be identical. This is true for both free slumping (in the absence of a mould) and slumping that is influenced by mould contact. This means that the dimensionless problem (for constant $\mu = 1$) can be solved once to give the shape of the slumping item over dimensionless time. The outcome for different viscosity (i.e. temperature) profiles and real times can then be determined by computing the equivalent dimensionless time as a post-processing operation, and selecting the slumped shape corresponding to this time.

4 Numerical Slumping — An Example

To illustrate the methods outlined above, let us consider an axisymmetric arrangement of an initially-flat glass disc, of radius a and thickness h such that $h/a = 0.1333$, supported on a concave mould, of radius a and centre depth δ_m such that $\delta_m/a = 0.0946615$, as shown in Figure 3. For clarity the vertical scale is twice the horizontal scale. For this problem, the axisymmetric form of (1) and (2) are solved in the (r, z) plane, where $r \equiv x_1$ is the horizontal radial direction and $z \equiv x_3$ is directed vertically up. Let the radial and vertical velocity components be given by $(u, v) \equiv (u_1, u_2)$. Computations may be restricted to a radial cross-section of the disc-mould combination (i.e. $0 \leq r \leq a$), with the appropriate boundary conditions at $r = 0$ being a zero radial velocity component ($u = 0$) together with the no-stress conditions (4). The mould surface may have an aspheric profile, though for current

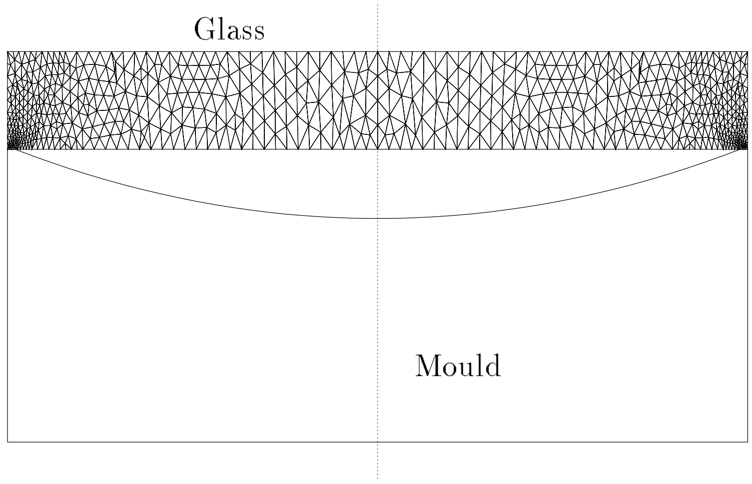

Figure 3: Geometry prior to slumping ($t = 0$)

purposes it has been chosen to be spherical in order to more clearly show the differences that slumping produces in the top free surface of the glass compared with the mould surface. The mould cavity is approximated by 21 equally spaced points connected by straight-lines, and has a small flat ledge of width $0.02a$ around its perimeter on which the glass disc is supported. A mesh of six-node triangles is defined over the glass domain. While the axisymmetry of the problem certainly simplifies the computations, a fully three-dimensional case can be readily solved, once the more difficult tasks of mesh generation for both mould surface and glass have been accomplished.

A non-uniform mesh element distribution has been used over the glass disc, with elements clustered in the region of the edge support where there

Table 1: Convergence with increasing numbers N_e of mesh elements shown by the initial vertical velocity v and pressure p at the centre of the top glass surface.

N_e	$-v/\mathcal{U}$	$p/\mathcal{P}$
332	4.639100	4.634920
415	4.648148	4.644334
505	4.652347	4.641609
600	4.651764	4.642715
697	4.651284	4.638801
792	4.652503	4.641972
890	4.652096	4.639168

is an initial pressure singularity. This has been found [16] to give much more rapid convergence with increasing numbers of mesh elements than does a mesh of uniformly spaced elements. Convergence of the finite-element method is demonstrated in Table 1. For the simulation discussed here, a mesh of 600 triangular elements has been used, which gives node velocities (and pressures) to at least three significant figures. Multiplying the node velocities by a time step gives the node displacements during that time step, from which the sag of the disc is obtained. Table 2 shows the vertical (z) coordinate at the centre of the top glass surface at $t = 0.016\mathcal{T}$ after initial contact of the centre of the lower glass surface with the mould (see Figure 4). Results computed using different values for (maximum) size of time step Δt^* and maximum node displacement $|\Delta\vec{x}^*|$ are given to demonstrate convergence

Table 2: Convergence with decreasing time step Δt^* and node displacement limit $|\Delta\vec{x}^*|$ as shown by the height at the centre of the top glass surface at $t = 0.016\mathcal{T}$.

Δt^*	$\lvert\Delta\vec{x}^*\rvert$	N_t	z^*
0.004	0.01	14	0.039863
0.002	0.01	18	0.039820
0.001	0.01	20	0.038951
0.0005	0.01	37	0.038884
0.0005	0.001	106	0.038846
0.0001	0.01	165	0.038839
0.0001	0.0001	971	0.038829

with increasing numbers N_t of time steps. (Asterisks denote dimensionless quantities.) Values of $\Delta t^* = 0.0005$ and $|\Delta\vec{x}^*| = 0.001$ give three figures of accuracy, and were used for the simulation illustrated in Figures 3 to 5. Note that during slumping after initial contact ($t > 0.016\mathcal{T}$), time steps and node displacements smaller than the specified maxima are typical to prevent nodes from passing through the mould surface, so that computational accuracy is better than in the stage up to initial mould contact.

Figures 3 to 5 show the progress of the glass slumping into the mould up to the point at which full mould contact is attained. Prior to full mould contact, slumping proceeds quite rapidly, though in real terms this may take in excess of 1 hour. Mould contact greatly reduces the rate of flow, and after full mould contact, slumping effectively ceases with further flow taking many

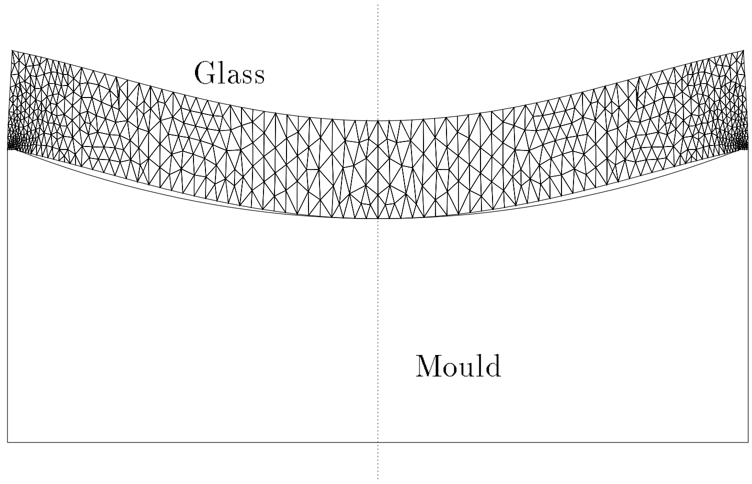

Figure 4: Initial mould contact at $t = 0.016\mathcal{T}$.

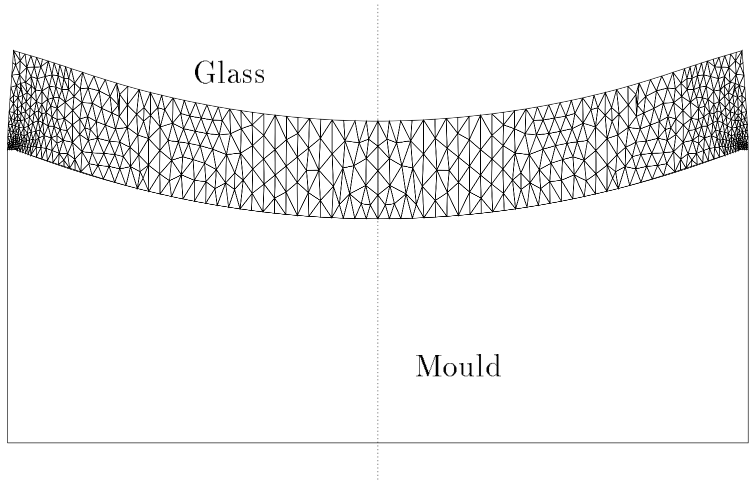

Figure 5: Full mould contact at $t = 0.075\mathcal{T}$

hours or even days.

Computation time for the whole simulation up to $t = 0.075\mathcal{T}$, when full mould contact between glass and mould has been achieved, was about 96 minutes using a direct Gauss-elimination banded-matrix solver and a single 167 MHz processor on a Sun Ultra Sparc 170 computer having 256MB of RAM.

Figure 5 does not show at optical accuracy, how well or poorly the mould surface has been replicated on the top glass surface. Hence we now look at determining surface curvature.

5 Surface Curvature

For optical surfaces, the design criterion is that the surface curvature meets the specification to within some tolerance. For the axisymmetrical example under consideration, the height z of the top glass surface is a function of radius r only and curvature κ is given by

$$\kappa = \frac{z''}{(1 + z'^2)^{3/2}} \tag{10}$$

where primes denote differentiation with respect to r. Coordinates (r, z) of nodes located on the top glass surface may be extracted from the finite-element output, from which first and second derivatives must be determined so as to compute the surface curvature profile.

The plainly difficult task of accurately differentiating non-exact data such as is obtained from any discretised computation process is an area of current research. Finite-difference methods for numerical differentiation of uniformly spaced data have received considerable attention over many years, and this is still an area of active investigation [1, 2]. An alternative to finite-difference techniques that is more suitable for non-uniformly spaced data such as in the present problem is to fit splines to the (r, z) data from which derivatives may be computed [6, 10]. The degree of the splines and the multiplicity of knots determine the extent of continuity and hence the order of derivatives that may be obtained. For data that is known to be non-exact and require smoothing, a least-squares fit is better than interpolation. Here, least-squares B-spline approximations are used, which are recommended by de Boor [6] as "very effective" for filtering noise from non-exact data. Multiple knots are permitted at the end points but not in the interior of the fitted curve, and B-splines of degree 4 or higher are used to ensure that the second derivative, and hence the curvature, is both continuous and differentiable, excepting at the end points of the curve. For adequate continuity and symmetry at $r = 0$ the

(r, z) coordinate data from the finite-element computations is mirrored in the $r = 0$ axis to give a data set across the full diameter of the glass component, to which the B-spline fit is made. The number of degrees of freedom (i.e. terms in the B-spline series) is determined by experiment. For best accuracy, it is desirable to have a large number of degrees of freedom, but not so large that the curvature is affected by error in the data [6]. Internal knots are uniformly spaced across the diameter. This method of computing curvature may also be extendible to three-dimensional surfaces (see [6]), although this work has not yet progressed this far.

For the slumping simulation shown in Figures 3 to 5, the top glass surface is defined by 149 nodes across the diameter, and we consider the curvature profile of this surface at time $t = 0.075\mathcal{T}$, after the lower surface of the glass disc has attained full contact with the mould. The number of degrees of freedom D_f of the B-spline approximation was increased from 15, until instability in the curvature profile due to error in the coordinate data was seen. The process is illustrated for quartic B-splines in Figure 6. For $35 \leq D_f \leq 65$ the curvature profile barely changes, and for $D_f = 75$ fluctuations in the curve due to noise in the coordinate data can be seen. As shown in Figure 7 for $D_f = 35$, similar results are obtained with B-spline approximations of degrees

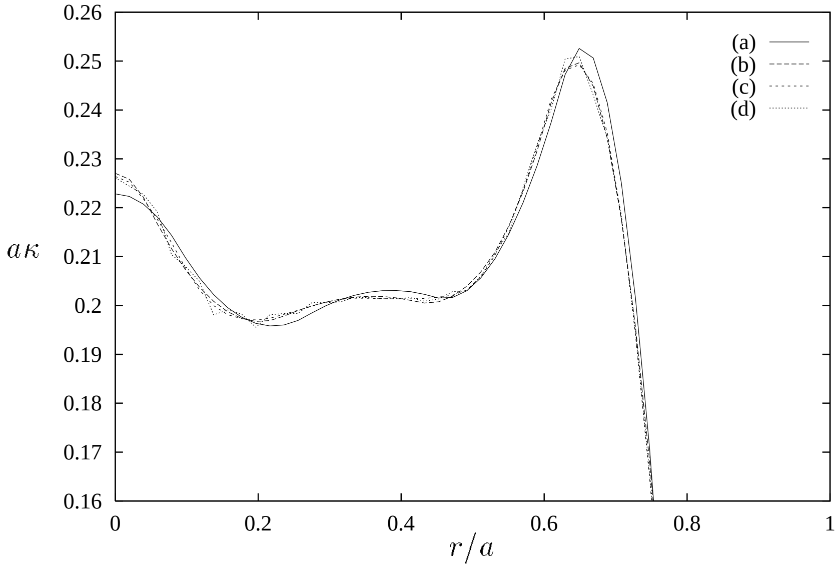

Figure 6: Determining surface curvature of the slumped disc of Figure 5 using quartic B-spline approximations. (a) $D_f = 15$, (b) $D_f = 25$, (c) $35 \leq D_f \leq 65$, and (d) $D_f = 75$.

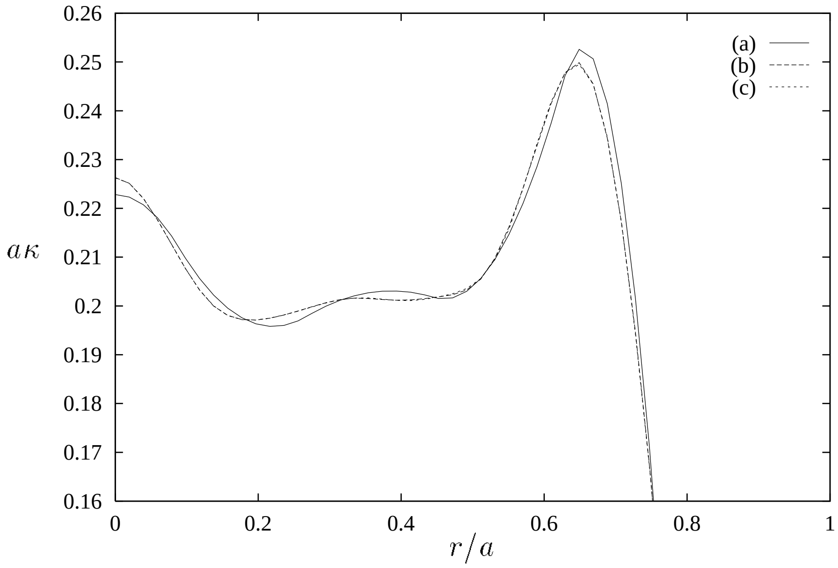

Figure 7: Surface curvature of the slumped disc using B-spline approximations of degree (a) 4, (b) 5, and (c) 6.

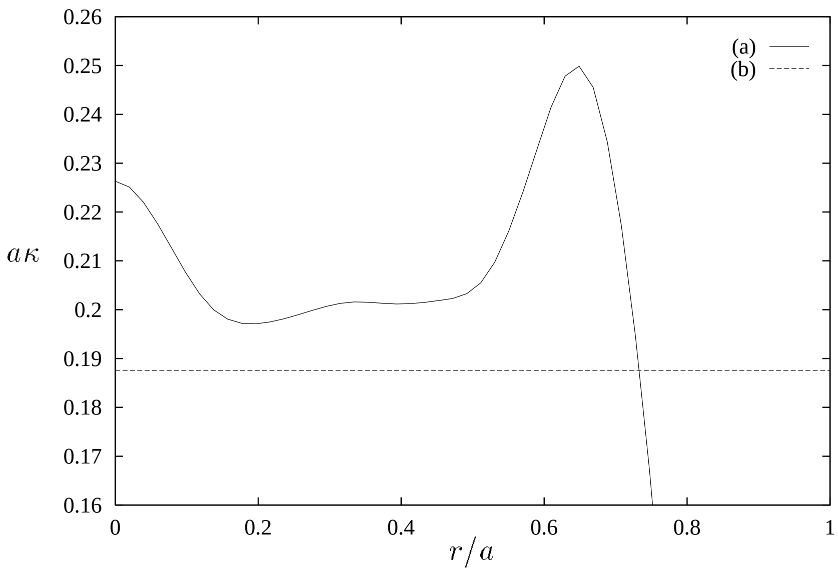

Figure 8: Curvature profiles of (a) the slumped glass disc at $t = 0.075\mathcal{T}$ (solid curve) and (b) the mould surface (dashed line).

4, 5 and 6, with the profiles obtained from the two highest degree B-spline approximations being virtually identical. Because of this it is concluded that the curve obtained from a quintic B-spline approximation with 35 degrees of freedom is the curvature profile of the slumped glass disc. This profile is shown again as the solid curve in Figure 8. Also shown, as the dashed line, is the constant curvature $a\kappa = 0.1876$ of the mould surface.

Further work is required to determine whether this method of computing the surface curvature of a slumped glass disc gives the profile to within permissible optical tolerances, which for the present example in the context of ophthalmic lens mould manufacture is estimated to be around $\pm 0.001/a$. However, it is clear from the results presented that, even allowing for error in curvature calculation, the actual slumped profile differs substantially from the mould curvature being 'replicated' by amounts well in excess of possible computational error, and we could proceed immediately to modify the mould surface so as to more nearly obtain the desired spherical optical surface.

It is possible that curvature might be more efficiently computed with a non-uniform distribution of the internal knots such that there is a greater knot density in regions of rapid change in curvature, but we can be satisfied with the accuracy of the results obtained with uniformly spaced knots since they remain basically unchanged over a large range of degrees of freedom of the B-spline approximations and hence knot density. Some experimenting with Chebyshev knot spacing showed this to be inappropriate for this data, leading to problems with matrix invertibility. By contrast uniform spacing is very reliable in giving a solvable problem, and the price of any lack in computational efficiency is small, especially when compared with the computational time that can be spent in searching for some better knot distribution.

It is of interest to see the dependence of the curvature profile on the discretisation used in the finite-element computations. Since the method

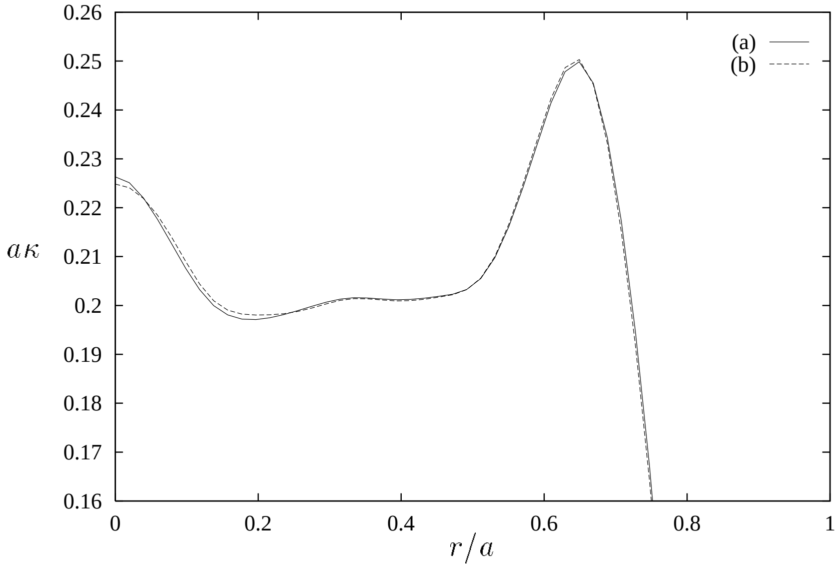

Figure 9: Curvature profile for the slumped glass disc (a) as computed previously, and (b) computed from a numerical simulation with a coarser mesh and larger time steps.

of calculating curvature filters noise from the data it may be possible to find the curvature profile sufficiently accurately from a less accurate and computationally cheaper finite-element simulation using a coarser mesh and larger time steps. Figure 9 compares the curvature profile of Figure 8 with that computed from a simulation using a mesh of 415 elements, a maximum time step of $\Delta t^* = 0.001$, and a maximum node displacement of $|\Delta \vec{x}^*| = 0.01$. This latter simulation up to full mould contact took about 15 minutes compared with 96 minutes for the previous more accurate simulation. Both curves were computed from a quintic B-spline approximation with 35 degrees of freedom. Both of these curvature profiles agree extremely well, and at this stage of this work curve (a), although derived from a simulation using a finer mesh and smaller time steps, cannot be considered to be more accurate than curve (b). This gives increased confidence in least-squares B-spline fitting as a satisfactory method for obtaining quite accurate curvature profiles from non-exact discrete data.

6 Conclusion

Numerical tools have been developed to simulate the slumping of molten glass into an axisymmetric mould that may have an aspheric profile, and to compute the curvature of the resulting top free surface. Their use has been demonstrated for a flat glass disc slumping into a spherical mould, showing that the mould surface is not replicated to optical accuracy. Simulation work could be continued to iteratively determine the mould profile that will yield the required free surface.

As discussed earlier in this paper, there are issues of spatial uniformity of temperature and viscosity that need to be considered when developing tools for numerically simulating glass-forming processes. The model and solution techniques described here are readily extended to include prescribed spatial temperature/viscosity variations throughout the glass, and this has been done in [16]. Some preliminary comparisons of isothermal and selected non-isothermal simulations with experimental results have also been conducted [15], which show good qualitative agreement when using an isothermal numerical model as here presented.

7 Acknowledgments

I am grateful to Dr S. Elhay, Department of Computer Science, University of Adelaide, for his very helpful suggestions and comments relating to the B-spline calculation of curvature, and to my supervisor Professor E.O. Tuck for his direction and assistance throughout the course of this work. I also acknowledge the support of an APA (Industry) scholarship. Finite-element mesh generation was done using the automatic mesh generation facility of the CFD package *Fastflo*, developed by the CSIRO Division of Mathematics and Statistics, Australia.

References

[1] Anderssen, R.S. and de Hoog, F.R., Finite difference methods for the numerical differentiation of non-exact data. *Computing*, 1984, **33**, 259–267.

[2] Anderssen, R.S., de Hoog, F.R., and Hegland, M., A stable finite difference ansatz for higher order differentiation of non-exact data. Mathematics Research Report MRR96-023, Centre for Mathematics and its Applications, Australian National University. Available at `http://discus.anu.edu.au:80/ marcus/litheg.html`

[3] Batchelor, G.K., *An Introduction to Fluid Dynamics*, Cambridge University Press, 1967.

[4] Burley, D.M. and Graham S.J., The blowing of thin films into moulds with applications in the glass container industry. *Math. Fin. Elem. and Appl.*, 1991, **7**, 279–286.

[5] Cormeau, A., Cormeau, I., and Roose J., Numerical simulation of glass-blowing. In J.F.T. Pittman, O.C. Zienkiewicz, R.D. Wood, and

J.M. Alexander (eds), *Numerical Analysis of Forming Processes*, John Wiley and Sons, Chichester, 1984, 219–237.

[6] de Boor, C., *A Practical Guide to Splines*, Applied Mathematical Sciences Vol. 27, Springer-Verlag, 1978.

[7] Graham, S.J., Burley, D.M., and Carling, C.J., Fluid flow in thin films using finite elements. *Math. Engng Ind.*, 1992, **3**, 229–246.

[8] Gulati, S.T., Fontana, E.H., and Plummer, W.A., Disc bending viscometry. *Phys. and Chem. of Glasses*, 1976, **17**, 114–119.

[9] Howell, P.D., Models for thin viscous sheets. *Euro. Jnl of Applied Math.*, 1996, **7**, 321–343.

[10] Norton, A.H., The use of convolution splines in the NQS Einstein evolution code. In B.J. Noye, M.D. Teubner, and A.W. Gill (eds), *Computational Techniques and Applications: CTAC97.* World Scientific, Singapore, 1998, 473–480.

[11] Pittman, J.F., Zienkiewicz, O.C., Wood, R.D., and Alexander, J.M. (eds), *Numerical Analysis of Forming Processes*, John Wiley and Sons, Chichester, 1984.

[12] Pollicove, H.M., Survey of present lens molding techniques. In M.J. Riedl (ed), *Replication and Molding of Optical Components*, Vol. 896, Proceedings of The Society of Photo-Optical Instrumentation Engineers. Washington; Bellingham, 1988, 158–159.

[13] Scholze, H. and Kreidl, N.J., Technological aspects of viscosity. In D.R. Uhlmann and N.J. Kreidl (eds), *Glass Science and Technology*, Vol. 3 Viscosity and Relaxation, Academic Press, Orlando, 1986, 233–273.

[14] Smith, L., Tillen, R.J., and Winthrop, J., New directions in aspherics: glass and plastic. In M.J. Riedl (ed), *Replication and Molding of Optical Components*, Vol. 896, Proceedings of The Society of Photo-Optical Instrumentation Engineers. Washington; Bellingham, 1988, 160–166.

[15] Stokes, Y.M., Thermal replication: a comparison of numerical and experimental results. In E.O. Tuck and J.A.K. Stott (eds) *The Proceedings of the 3rd Biennial Engineering Mathematics and Applications Conference: EMAC98.* The Institution of Engineers, Australia, 1998, 471–474.

[16] Stokes, Y.M., *Very Viscous Flows Driven by Gravity with particular application to Slumping of Molten Glass.* PhD Thesis, University of Ade-

laide, July 1998.

[17] Tuck, E.O., Stokes, Y.M., and Schwartz, L.W., Slow slumping of a very viscous liquid bridge. *J. Eng. Math.*, 1997, **32**, 31–44.

[18] van de Fliert, B.W., Howell, P.D., and Ockendon, J.R., Pressure driven flow of a thin viscous sheet. *J. Fluid Mech.*, 1995, **292**, 359–376.

[19] Williams, J.H., Owen, D.R.J., and Sa, J.M.A.C., The numerical modelling of glass forming processes. *Collected papers, XIV Intl. Congr. on Glass*, 1986, 138–145.

List of Figures